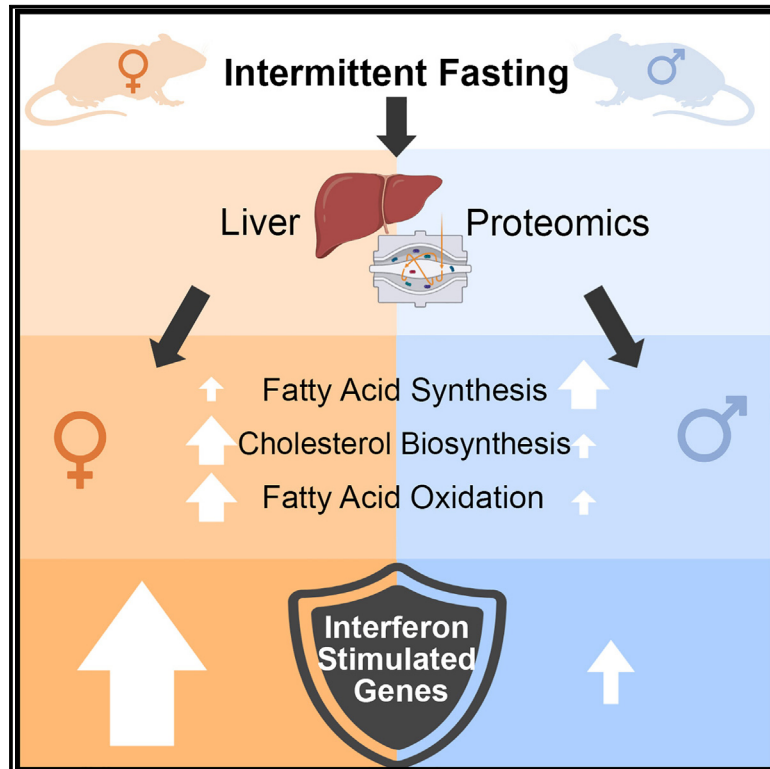


## Dietary restriction induces a sexually dimorphic type I interferon response in mice with gene-environment interactions

### Graphical abstract



### Authors

Dylan J. Harney, Michelle Cielech, Georgia E. Roberts, ..., Markus J. Hofer, Nadine Laguette, Mark Larance

### Correspondence

mark.larance@sydney.edu.au

### In brief

In this study, the effect of intermittent fasting is examined in the liver proteome of mice. Harney et al. observe a sexually dimorphic response in lipid metabolism pathways and type I interferon signaling. This response differs with gonadectomy. The magnitude of this response differs between mouse strains and environments.

### Highlights

- Intermittent fasting induces sexually dimorphic changes in the mouse liver proteome
- Females induce interferon-stimulated genes that require type I interferon secretion
- Gonadectomy shows the key role of ongoing sex hormone signaling in this effect
- The magnitude of the response changes with genetic background and environment



## Article

# Dietary restriction induces a sexually dimorphic type I interferon response in mice with gene-environment interactions

Dylan J. Harney,<sup>1</sup> Michelle Cielech,<sup>2</sup> Georgia E. Roberts,<sup>1</sup> Isabelle K. Vila,<sup>3</sup> Barney Viengkhou,<sup>1</sup> Markus J. Hofer,<sup>1</sup> Nadine Laguette,<sup>3</sup> and Mark Larance<sup>2,4,\*</sup>

<sup>1</sup>Charles Perkins Centre and School of Life and Environmental Sciences, The University of Sydney, Sydney, 2006 NSW, Australia

<sup>2</sup>Charles Perkins Centre and School of Medical Sciences, The University of Sydney, Sydney, 2006 NSW, Australia

<sup>3</sup>IGMM, Université de Montpellier, CNRS, Montpellier, France

<sup>4</sup>Lead contact

\*Correspondence: [mark.larance@sydney.edu.au](mailto:mark.larance@sydney.edu.au)

<https://doi.org/10.1016/j.celrep.2023.112559>

## SUMMARY

Intermittent fasting (IF) is an established intervention to treat the growing obesity epidemic. However, the interaction between dietary interventions and sex remains a significant knowledge gap. In this study, we use unbiased proteome analysis to identify diet-sex interactions. We report sexual dimorphism in response to intermittent fasting within lipid and cholesterol metabolism and, unexpectedly, in type I interferon signaling, which was strongly induced in females. We verify that secretion of type I interferon is required for the IF response in females. Gonadectomy differentially alters the every-other-day fasting (EODF) response and demonstrates that sex hormone signaling can either suppress or enhance the interferon response to IF. IF fails to potentiate a stronger innate immune response when IF-treated animals were challenged with a viral mimetic. Lastly, the IF response changes with genotype and environment. These data reveal an interesting interaction between diet, sex, and the innate immune system.

## INTRODUCTION

Sex has a profound influence on many aspects of biology including behavior, metabolism, immunity, and aging.<sup>1–5</sup> For example, women have lower fasting glucose levels but a larger area under the curve for an oral glucose tolerance test compared with men.<sup>6</sup> Both the innate and adaptive immune responses differ significantly between the sexes, with females having increased protection from viral infections<sup>7</sup> but an increased risk of developing autoimmune disease and adverse immunological reactions.<sup>7,8</sup> Metabolic disease risk is also sexually dimorphic, with significantly fewer pre-menopausal women having type 2 diabetes<sup>9</sup> and non-alcoholic fatty liver disease (NAFLD)<sup>10</sup> compared with men.

Intermittent fasting (IF) is a dietary intervention that has been shown to provide metabolic benefits alongside other phenotypes such as altering immune cell populations.<sup>11–14</sup> Rodent models have been pivotal in understanding IF and determining the molecular mechanisms underlying these beneficial effects, with research focusing on key fasting-responsive tissues such as liver and adipose.<sup>11–17</sup> However, such rodent studies have been restricted to males, significantly limiting our understanding of sex-regulated mechanisms in the response to IF. This is somewhat abrogated in human studies, where male and female peripheral tissue has been examined for alterations in gene expression.<sup>16–20</sup> However, without knowing how protein abundance

changes during IF in key organs such as the liver, many of the underlying molecular mechanisms remain unknown. Conversely, sexually dimorphic responses have been observed in chronic calorie restriction (CR), where 20% CR extends the lifespan in female mice but not male mice.<sup>21</sup> Furthermore, several publications have highlighted sexually dimorphic responses to endocrine stimuli in the liver<sup>22–24</sup>; thus, the response to IF is likely to be similarly affected by sex.

To identify key pathways and networks that are sexually dimorphic in response to IF, we performed an unbiased comparison of the response to IF in male and female livers of mice with high resolution mass-spectrometry-based proteomics. Using the every-other-day fasting (EODF) diet model, we showed that EODF improves the metabolic health of both sexes and induces sexually dimorphic metabolic changes in lipid synthesis and catabolism. Surprisingly, EODF induced a strong up-regulation of anti-viral interferon-stimulated gene (ISG) products in female livers with a much weaker response in males. This response was dependent on secreted type I interferon, as an intact receptor was required for the response. We demonstrated that ongoing testosterone signaling was required to suppress the IFN response in male animals. Conversely, removal of estrogen signaling reduced the abundance of ISG proteins but did not inhibit the EODF response. We demonstrated that the magnitude of this response was significantly altered by genetic and environmental conditions. Lastly, when EODF-treated mice were



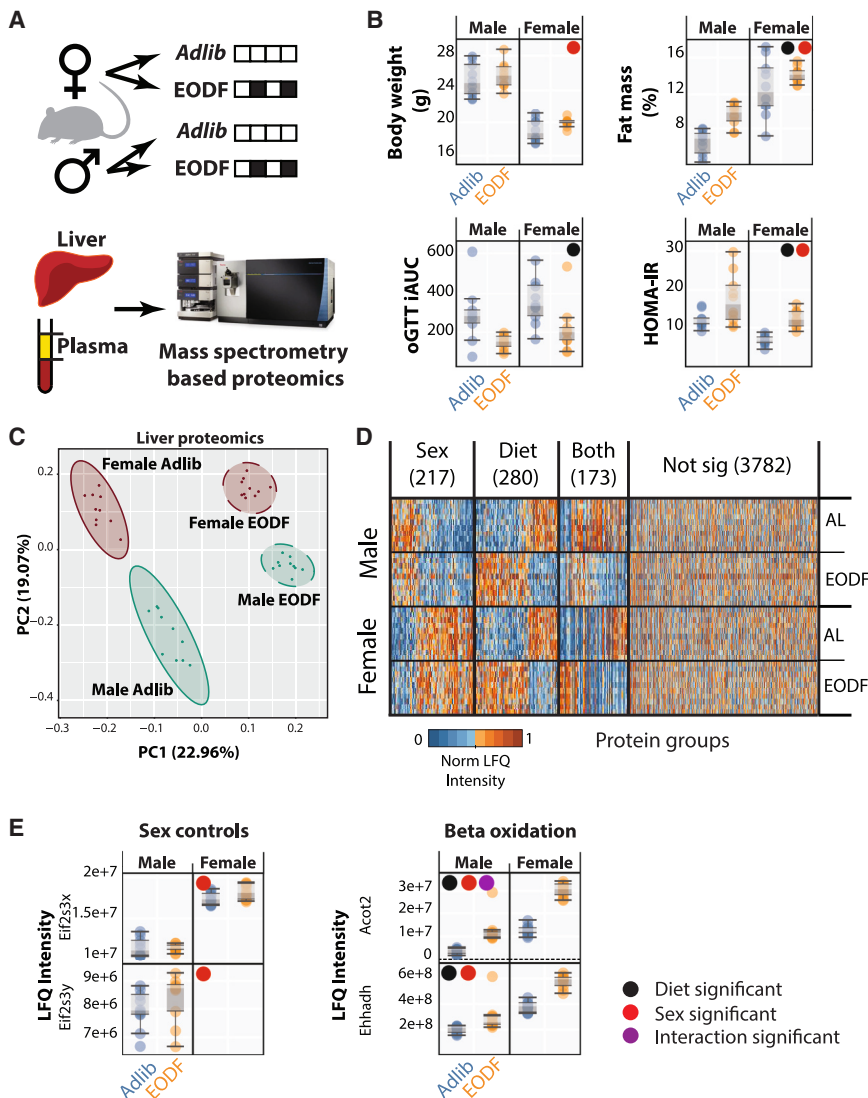


**Figure 1. EODF model improves metabolic health in both male and female mice**

(A) Male and female C57BL/6J mice at 8 weeks of age were given either *ad libitum* or EODF food access for 2 weeks, and their organs were harvested after 2 weeks on LN<sub>2</sub> and subjected to tandem mass spectrometry. *n* = 10 per treatment group.

(B) Boxplots were generated for physiological data, where each circle is an individual animal, and the box represents 95% confidence intervals and whiskers represent 1.5x interquartile range.

(C and D) Liver tissue was analyzed by mass spectrometry, and proteins detected in every animal were subjected to (C) principal-component analysis (PCA) and (D) were plotted in a heatmap where each column is an individual animal. LFQ intensities were normalized to between 0 and 1 on a per-gene basis.

(E) These proteins were plotted individually where each circle is an individual animal, and the boxes represent 95% confidence intervals and whiskers represent 1.5x the interquartile range. Significance was determined as *p* < 0.05 by two-way ANOVA after Benjamini-Hochberg correction.

challenged with a viral mimetic, there was no potentiation of the innate immune response by EODF. Together this comprehensive analysis of diet-sex interactions across the liver proteome provides an insight into type I interferon-lipid metabolism mechanisms and highlights key areas for further analysis.

## RESULTS

### EODF improves metabolic health and stimulates metabolic proteomic changes in the liver

To identify key pathways and networks that are sexually dimorphic in response to IF, both male and female C57BL/6J mice were subjected to 2 weeks of either *ad libitum* feeding or an EODF diet (Figure 1A). Male and female mice showed similar physiological responses to the EODF intervention, including body weight, fat mass, fasting glucose, oral glucose tolerance testing (oGTT) area under the curve (AUC), plasma ketones, and non-esterified fatty acids (NEFAs) (Figures 1B and S1). Female

mice fed *ad libitum* had consistently higher liver triacylglyceride levels, but this decreased following EODF (Figure S1). Unbiased mass-spectrometry-based proteomic analysis allows for comprehensive monitoring of cellular pathways and was applied to liver tissue from each animal. From this analysis, ~5,500 proteins (Table S1) were identified. The label-free quantification (LFQ) normalized intensities of these proteins were used in a principal-component analysis (PCA), which illustrated consistency within treatment groups through a strong diet separation in the first component (x axis) and sex separation in the second component (y axis) (Figure 1C). All proteins were subjected to a two-way ANOVA and subsequent Benjamini-Hochberg correction to detect EODF-dependent effects, sex-dependent effects, or interactions between these variables. This allowed detection of 280 EODF-responsive proteins, 220 sex-responsive proteins, and 170 proteins showing a significant interaction between sex and diet (Figure 1D). As positive controls for sex differences, we confirmed that proteins encoded by sex chromosome-specific genes, eukaryotic translation initiation factor 2 subunit 3 X and Y linked (Eif2s3x and Eif2s3y), showed the expected abundance variations (Figure 1E).

### EODF induces sexually dimorphic changes in numerous metabolic pathways

Based upon our previous studies in male mouse liver, representative EODF-responsive proteins involved in fatty acid catabolism, acyl-coenzyme A thioesterase 2 (ACOT2) and peroxisomal bifunctional enzyme and (EHHADH), were examined. Both

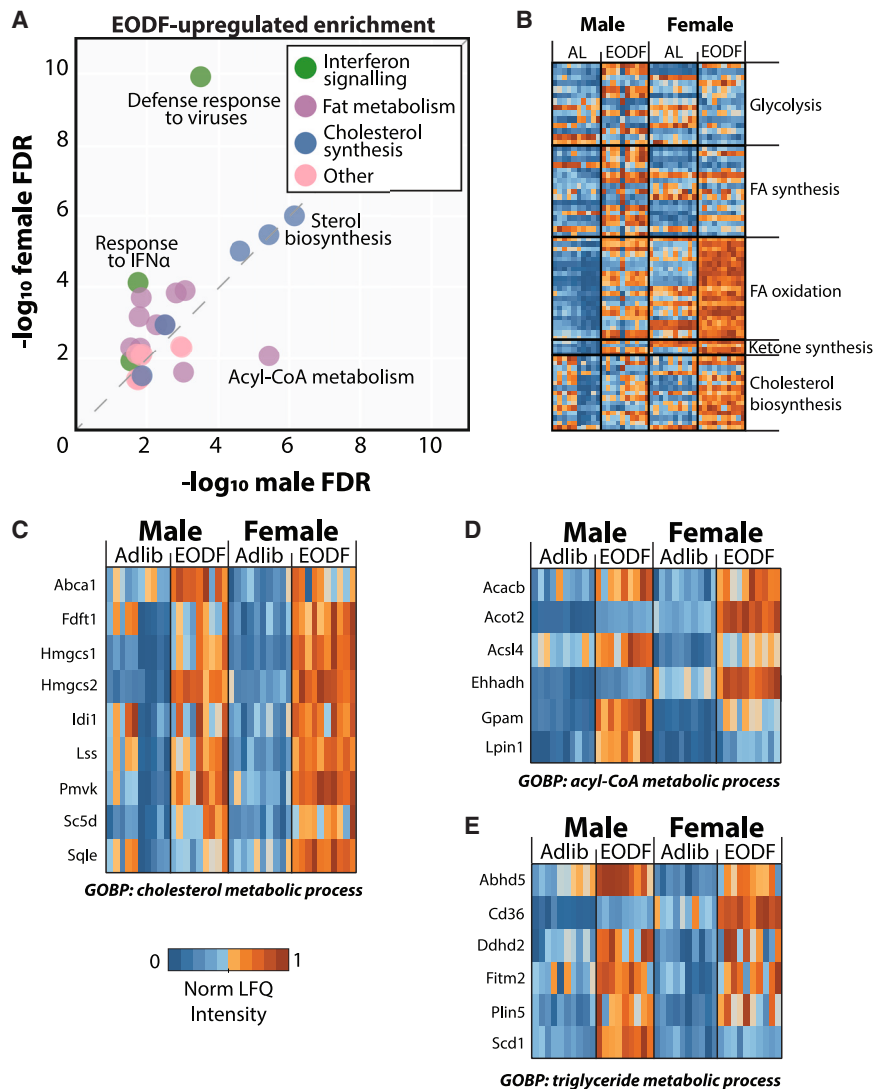


**Figure 2. Pathway enrichment reveals that EODF induces changes in fatty acid metabolism in a sexually dimorphic manner**

(A) Protein fold changes in mouse liver between EODF/*ad libitum* were subject to pathway enrichment in STRING where each circle represents an individual pathway based on enrichment score. (B) Fasting-responsive metabolic pathways were plotted in a heatmap, and LFQ intensities were normalized between 0 and 1 on a per-gene basis. Each column represents an individual animal. (C–E) Proteins from enriched pathways were plotted based on GO-term biological pathways together in a heatmap where each column is an individual animal, and LFQ intensities were normalized to between 0 and 1 on a per-gene basis.

ACOT2 and EHHADH were upregulated in male mice as seen previously<sup>11</sup> (Figure 1E), but both displayed a much greater increase in abundance in females. Conversely, key proteins in fatty acid synthesis, acetyl-coenzyme A (CoA) carboxylase 1 (ACACA) and fatty acid synthase (FASN), were increased in males, as previously demonstrated,<sup>11</sup> but were much less responsive to EODF in females.

To detect differences in pathway utilization between the sexes in an unbiased manner, we used the STRING-db resource<sup>25</sup> for pathway enrichment analysis of the significantly upregulated proteins after EODF in both sexes (Figure 2A; Table S2). All detected proteins within these key metabolic pathways were plotted (Figure 2B). Males displayed a larger increase in glycolytic pathways compared with females after EODF, with females upregulating ketone synthetic pathways more than males. The increase in ketone synthesis fits with our observation that females had lower blood ketone levels, suggesting a higher utilization of this energy source (Figure S1). Previously, we have shown that EODF increases

cholesterol biosynthetic pathways in males,<sup>11</sup> but here we observe that females have a consistently higher abundance of proteins involved in the cholesterol biosynthetic pathway compared with males after EODF (Figure 2C). Fatty acid synthesis enzymes were increased in abundance in males more than females in response to EODF. For example, males on EODF displayed an increased abundance of 1-acylglycerol-3-phosphate O-acyltransferase (ABHD5), glycerol-3-phosphate acyltransferase 1 (GPAM1), phosphatidate phosphatase (LPIN1), and stearoyl-CoA desaturase (SCD1) (Figures 2D and 2E). Conversely, proteins involved in lipid catabolism were upregulated after EODF more strongly in females, including EHHADH, ACOT2, and scavenger receptor class b member 1 (CD36). Plasma was harvested from the same animals and subjected to untargeted

plasma proteomic analysis.<sup>16</sup> Many proteins well known to be sexually dimorphic in mice were observed, including the male pheromone major urinary proteins (MUPs) (Figure S2A). Interestingly, many proteins involved in innate immunity and inflammation including complement proteins and serum amyloid proteins were significantly decreased by EODF in both sexes (Figure S2B). There was also an increase in the abundance of apolipoproteins in both sexes including ApoA4, which has been observed previously.<sup>16</sup> Lastly, the adipose-secreted, insulin-sensitizing hormone adiponectin<sup>26</sup> was increased in both sexes after EODF, with females having higher levels of adiponectin in the *ad libitum*-fed animals (Figure S2B).

**IFN $\alpha$  signaling is strongly induced by EODF in females**

Unexpectedly, enrichment analysis of EODF-induced proteins showed that the IFN $\alpha$  signaling pathway was highly enriched in females, with only minor enrichment in males. As an extracellular warning signal, type I interferons such as IFN $\alpha$  and IFN $\beta$  engage

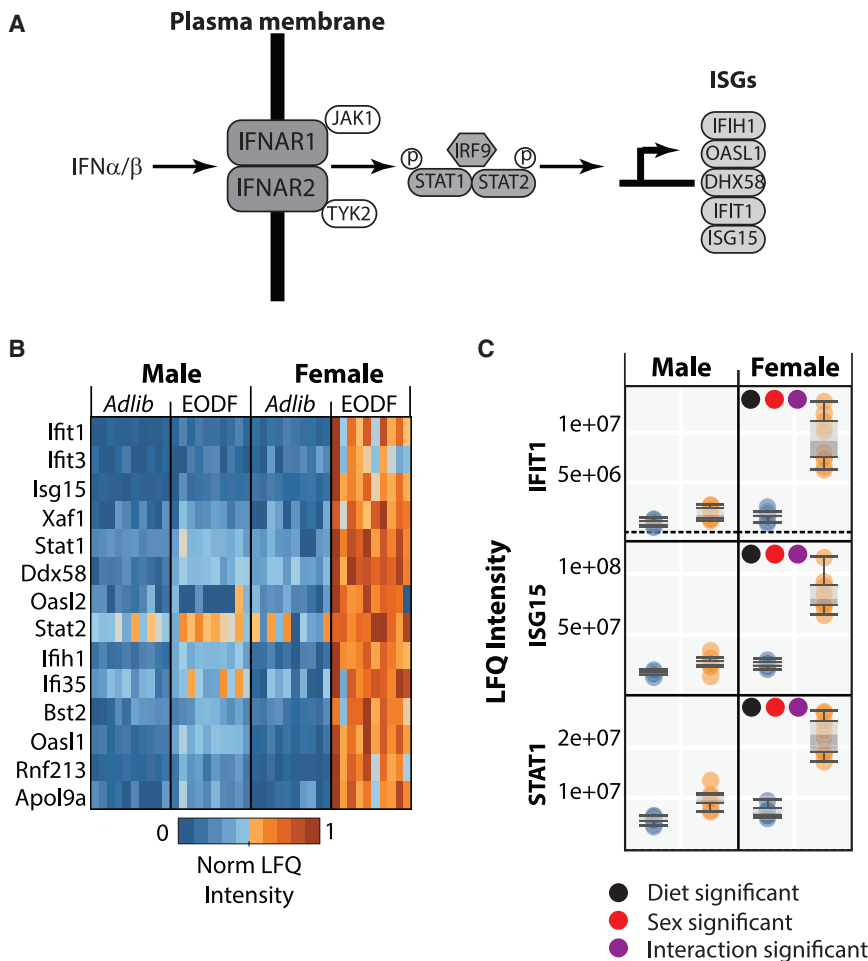


**Figure 3. EODF induces interferon  $\alpha$  (IFN $\alpha$ ) signaling in female but not male mice**

(A) A basic schematic showing the pathway downstream of IFN $\alpha/\beta$  production leading to ISG expression.

(B) Proteins known to be downstream of IFN $\alpha/\beta$  signaling were plotted together in a heatmap where each column is an individual animal, and LFQ intensities were normalized to between 0 and 1 on a per-gene basis.

(C) Some of these proteins were plotted individually, where each circle is an individual animal, and the boxes represent 95% confidence intervals and whiskers represent 1.5 $\times$  the interquartile range. Significance was determined as  $p < 0.05$  by two-way ANOVA after Benjamini-Hochberg correction.

their cognate heterodimeric receptors (IFNAR1-IFNAR2) on the cell surface, which triggers signal transducer and activator of transcription 1 (STAT1) activation and subsequent transcription of the ISG repertoire (Figure 3A).<sup>27</sup> Each protein downstream of IFN $\alpha/\beta$  signaling was examined and this revealed no changes between the sexes in *ad libitum*-fed animals (Figure 3B). Strikingly, EODF induced a large increase in abundance for many of the ISG proteins in females (e.g., ISG15, IFN-induced protein with tetratricopeptide repeats 1 [IFIT1], and 2'-5'-oligoadenylate synthase-like protein 1 [OASL1]), whereas males had a much weaker response (Figure 3C).

#### IFNAR1 knockout abrogates EODF-induced IFN $\alpha$ signaling

To determine if IFN $\alpha/\beta$  secretion is required for the observed EODF response, mice that were either wild type or IFNAR1-null (knockout [KO]) and unable to respond to IFN $\alpha/\beta$  were examined after an EODF intervention (Figure 4A). Comparing the physiological response to EODF between wild-type and KO mice showed no significant differences between the genotypes in both sexes (Figure S2). Proteome analysis of the livers from these animals was used to characterize the response (Table S1). A PCA of these data demonstrated a clear separation

regulation of ISGs in WT females, while the males showed a much weaker response (Figures 4C and 4D). The induction of ISGs was completely abolished by KO of IFNAR1 in both sexes, suggesting that IFN $\alpha/\beta$  secretion is required for the EODF-induced IFN signaling response.

#### Gonadectomy alters EODF-induced IFN $\alpha$ signaling

To test if androgen signaling has a key regulatory role in the ISG response, male mice were castrated at 5 weeks of age to remove ongoing sex hormone signaling and were examined in the EODF diet model (Figure 5A). Comparison of castrated and sham-operated animals showed that castrated males had higher fat mass but similar fasting blood glucose and a lower oGTT integrated area under the curve (iAUC) (Figure S4). The livers of these animals were analyzed by proteomics (Table S1) and the major fasting-responsive metabolic pathways examined (Figure 5B). Examining the proteomics output, we found that 758 proteins were significantly changed by diet, 980 were changed by castration, and 640 were changed by an interaction of both variables. Interestingly, castration increased the abundance of proteins involved in both fatty acid oxidation and ketone synthesis, making the castrated male response similar to that of female mice. Plotting the

of animal groups by sex and diet (Figure 4B). However, no significant separation was observed between wild-type and KO mice in any combination of diet-sex, suggesting that apart from a defect in the IFN $\alpha/\beta$  response, these animals were otherwise normal. Examining the proteomics output, 3,264 proteins were significantly changed by diet, 2,359 were changed by genotype, and 3,618 were changed by sex. Key fasting-responsive metabolic pathways (Figure 4C) were then plotted in a heatmap, which demonstrated very few differences between the wild-type (WT) and KO animals. Conversely, IFN $\alpha/\beta$ -induced proteins showed a strong EODF-induced up-

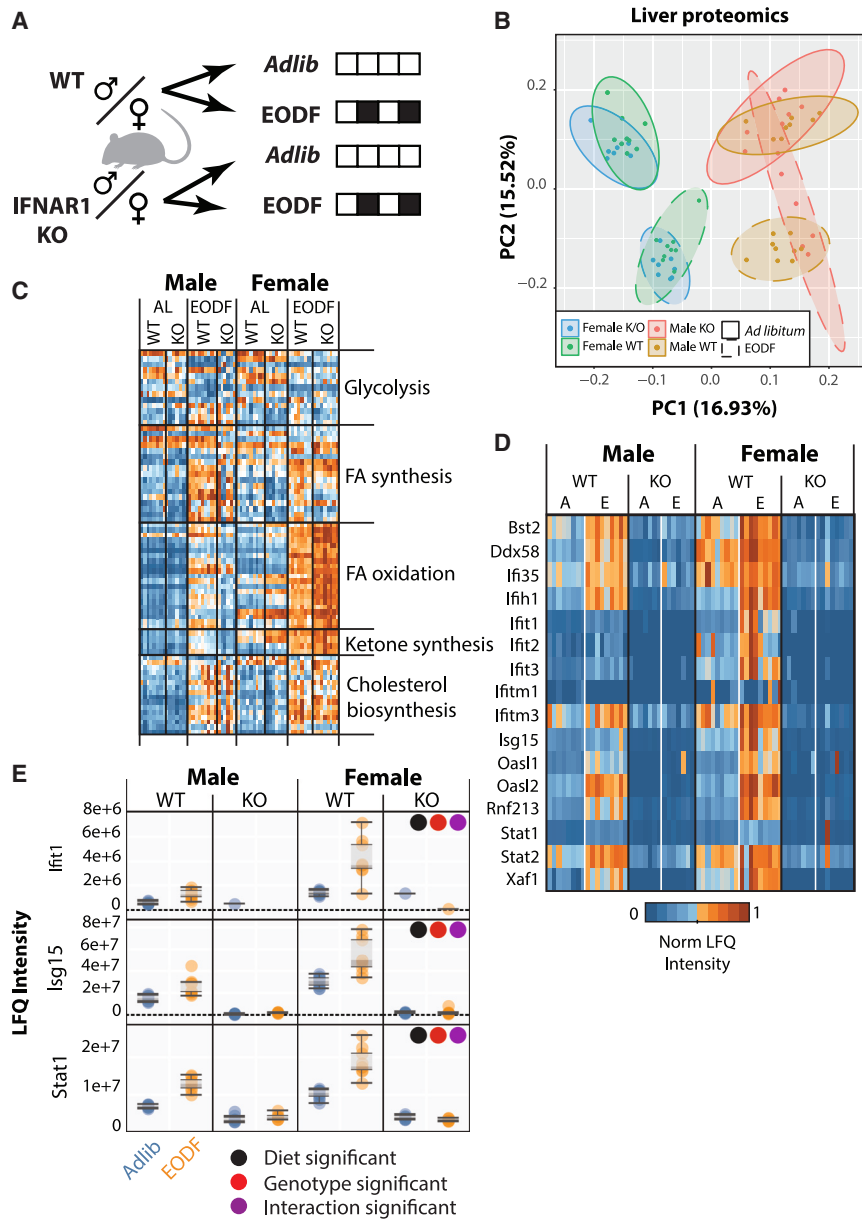


**Figure 4. Global IFNAR1 KO abrogates EODF-induced IFN $\alpha$ / $\beta$  signaling in mouse liver**

(A) Wild-type (8 male and 9 female AL, 9 male and 9 female EODF) and global IFNAR1 KO (7 male and 7 female AL, 7 male and 8 female EODF) male and female C57BL/6J mice at 8 weeks of age were given either *ad libitum* or EODF food access, and their organs were harvested after 2 weeks on LN<sub>2</sub> and subjected to tandem mass spectrometry.

(B) Proteins that were detected in every sample were subjected to PCA, where each circle represents an individual animal.

(C) Fasting responsive metabolic pathways were plotted in a heatmap, and LFQ intensities were normalized between 0 and 1 on a per-gene basis. Each column represents an individual animal.

(D and E) Proteins involved in IFN $\alpha$ / $\beta$  were plotted (D) in a heatmap where each column is an individual animal or (E) individually, and LFQ intensities were normalized to between 0 and 1 on a per-gene basis. Significance was determined as  $p < 0.05$  by three-way ANOVA after Benjamini-Hochberg correction. Error bars represent 1.5 times the interquartile range.

metabolic pathways were examined (Figure 5C). Examining the proteomics output, we found that 1,422 proteins were significantly changed by diet, 295 were changed by ovariectomy, and 10 were changed by interaction. The most significant difference induced by ovariectomy was in the cholesterol biosynthesis pathway, which was increased by EODF in the sham animals much more than the ovariectomized animals. Key ISG proteins had significantly lower abundance in the ovariectomized animals regardless of diet (Figure 5E). However, despite the lower abundance, the ovariectomized animals had a similar fold change of ISG protein induction following EODF. This suggests that estrogen signaling contributes to ISG protein

abundance but does not coordinate the EODF induction of IFN $\alpha$  signaling. To further elucidate the effects of gonadectomy on the liver proteome, some of the most changing proteins from each surgery were plotted (Figure 5F). After ovariectomy, proteins involved in IFN $\alpha$ / $\beta$  signaling (Rnf213 and Oasl1) and cholesterol biosynthesis (Sqli, Pmvk, and Fdft1) were the most decreased with EODF. The magnitude of this decrease was much larger than any increases in protein abundance, with no clear pathways enriched. In castrated animals, the most decreased proteins after EODF were involved in IFN $\alpha$ / $\beta$  pathway regulation (Irf2), autophagy (Map1lc3a), and proliferation (Egfr). The increased proteins were involved in diverse pathways including insulin signaling (Pdk1) and fatty acid oxidation (Acot2).

abundance of IFN $\alpha$ -regulated proteins showed that castration increased the abundance of ISG proteins (Figure 5D) in the *ad libitum*-fed castrated animals. The abundance of the ISG proteins was increased further by EODF, but this increase was small and statistically insignificant.

To examine how estrogen signaling may affect the EODF response, sham and ovariectomized animals underwent the EODF diet. Comparing the physiological response to EODF, the ovariectomized animals had lower fasting blood glucose and higher fasting blood insulin compared with the sham animals (Figure S4). The ovariectomized animals had higher fat mass than their sham counterparts, with reduced glucose tolerance regardless of diet. The livers of these animals were subjected to proteomic analysis (Table S1), and the key fasting-responsive

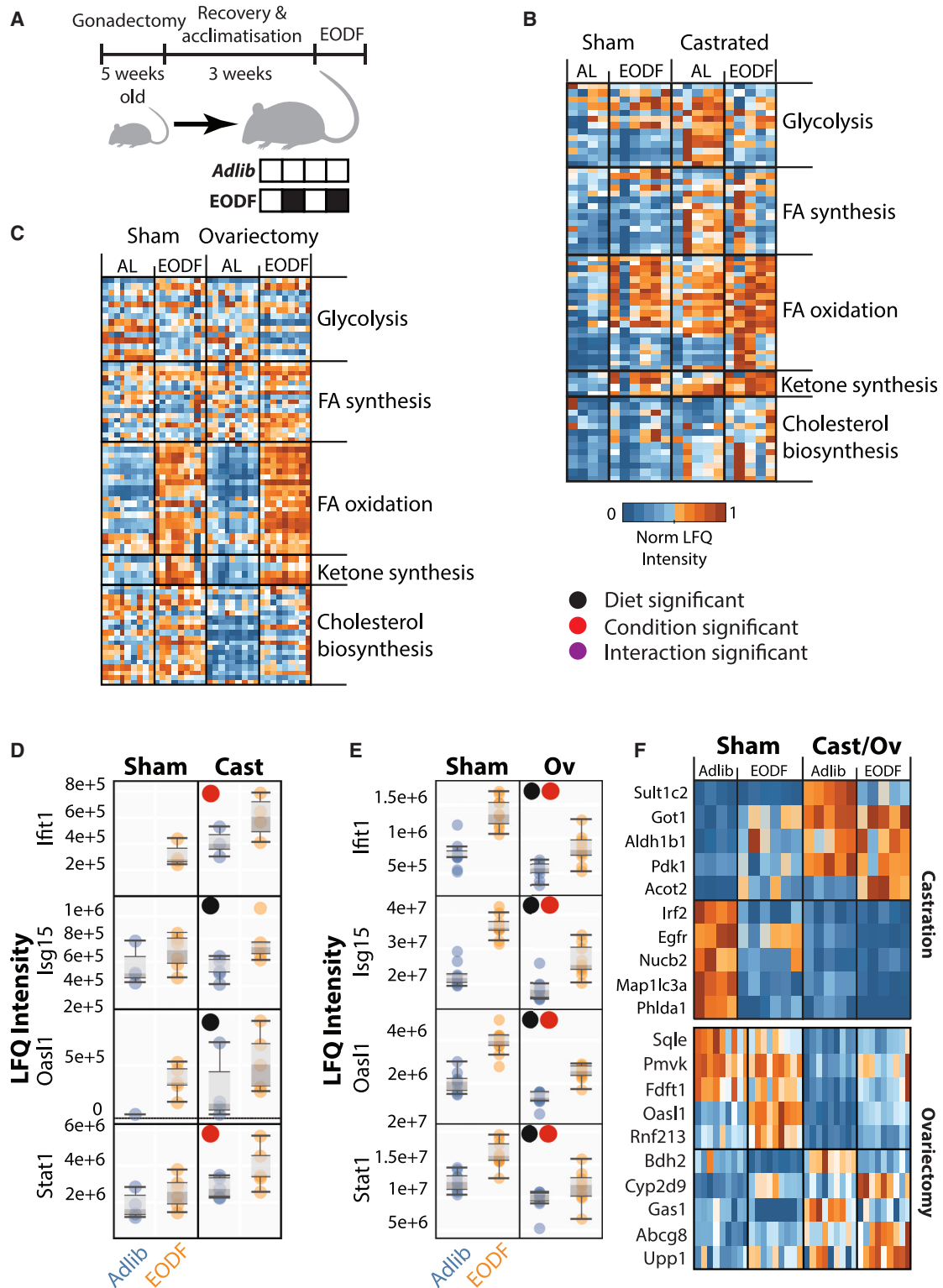


**Figure 5. Castration and ovariectomy differently modify the EODF-induced IFN $\alpha/\beta$  response**

(A) Male or female C57BL/6J mice at 5 weeks of age were castrated (cast) or ovariectomized (ov) and at 8 weeks of age were given either *ad libitum* (5 sham, 4 cast and 5 sham, 5 ov) or EODF (5 sham, 6 cast and 5 sham, 5 ov) food access, and their organs were harvested after 2 weeks on LN<sub>2</sub> and subjected to tandem mass spectrometry.

(legend continued on next page)

### EODF-induced IFN $\alpha$ signaling is altered by genetic and environmental conditions

To examine whether the IFN $\alpha$ / $\beta$  EODF response was specific to C57BL/6J mice, two strains of mice (C57BL/6J and BALB/c), which are genetically distinct, were subjected to EODF (Figure 6A). Their physiological response to EODF showed that the strains behaved similarly, with BALB/c mice having a small but significant decrease in fasting glucose and glucose tolerance (Figure S5). Alongside these differences, BALB/c mice had higher fat mass and gonadal fat weight compared with C57BL/6J, independent of sex (Figure S5). The livers of these mice were examined with proteomics (Table S1), and key fasting-responsive pathways were plotted (Figure 6B). Examining the proteomics output, we found that 807 proteins were significantly changed by diet, 1,129 were changed by strain, and 900 were changed by sex. One of the most striking changes was the induction of cholesterol biosynthesis pathways after EODF by C57BL/6J mice but not BALB/c mice. As observed in our previous experiments, males had higher fatty acid synthesis enzymes, while females had higher fatty acid oxidation enzymes, in both strains. BALB/c mice had a significant induction of ISG proteins after EODF that was much lower in magnitude than C57BL/6J mice (Figure 6C).

To examine the effect of the environment, C57BL/6J mice were subjected to EODF in a different laboratory in France (Figure 6D). The EODF regime used was identical, including time-of-harvest, with a similar diet (Table S4). This diet had a similar macronutrient balance compared with that used in Australia, with some differences in micronutrient content. In addition, the water supply was acidified in France, whereas it was not in all previous experiments. Overall, these animals showed similar physiological responses to EODF compared with previous experiments. Liver tissue from these animals was analyzed by proteome analysis (Table S1). Examining the proteomics output, we found that 1,943 proteins were significantly changed by diet, 2,030 were changed by sex, and 155 were changed by interaction. The key fasting-responsive pathways demonstrated significant overlap with the previous EODF experiments (Figure 6E). The proteomic response in females (France) was plotted against the female (Australia) data (Figure 6F). Both cohorts showed similar induction of fatty acid oxidation after EODF, but the mice in the French laboratory showed much lower induction of cholesterol biosynthetic enzymes. Interestingly, ISG proteins were induced after EODF in both cohorts, but the response was significantly lesser in the France cohort compared with the Australia cohorts.

### EODF does not potentiate IFN $\alpha$ signaling in mice given an innate immune challenge

We next wanted to determine if the EODF-mediated induction of IFN $\alpha$  could potentiate the response to a viral mimetic. Both

male and female C57BL/6J mice were subjected to the standard EODF regime. Following this period, mice were injected with either polyI:C, a viral mimetic, or a vehicle control, and tissues were harvested after 4 h (Figure 7A). Body temperature was taken rectally before, during, and after the treatment, which showed that in both sexes polyI:C significantly lowered the body temperature of *ad libitum* animals but not EODF animals (Figure 7B). Liver proteomics was performed (Table S1), and PCA plots of these data demonstrated a clear separation based on both diet and sex but not based on polyI:C injection (Figure 7C). Examining the proteomics output, we found that 2,949 proteins were significantly changed by diet, 447 were changed by injection, and 2,267 were changed by sex. Further examination of key fasting-responsive metabolic pathways demonstrated no differences between the vehicle- and polyI:C-injected animals (Figure 7D). However, ISG proteins were strongly induced by polyI:C injection. While EODF induced ISG proteins in females, there was no potentiation of ISG protein abundance by EODF when polyI:C was injected (Figure 7E). The only protein with potentiation was STAT1, the transcription factor responsible for the induction of ISG proteins.

### DISCUSSION

Here, we have highlighted the sexually dimorphic induction of the innate immune system through dietary restriction. This was made possible using an unbiased mass-spectrometry-based proteomics approach to examine livers of male and female C57BL/6J mice after EODF. Physiological analysis of both sexes revealed that EODF equally improved their metabolic health, but the sexes had a divergent metabolic response in liver tissue. Males induced fatty acid synthesis and glycolysis pathways in response to EODF, whereas females strongly induced fatty acid oxidation alongside higher cholesterol and ketone biosynthesis enzymes. Strikingly, ISG proteins were highly induced in livers from female animals after EODF, and this response required secretion of type I interferon and signaling through its cognate receptor. Castration perturbed this phenotype, causing male mice to have more female-like high ISG protein levels, whereas ovariectomy significantly dampened ISG protein abundance in females. Interestingly, this IFN $\alpha$ / $\beta$  response was lower in BALB/c mice and was drastically affected by environmental stimuli. EODF did not potentiate a stronger IFN $\alpha$ / $\beta$  response when mice were challenged with a viral mimetic. Together, this study provides an analysis of liver tissue from male and female mice subjected to IF and provides insight into the molecular mechanisms governing a diet-sex-immune interaction. These data are provided as an online resource through an interactive visualization for the research community (<https://www.larancelab.com/gendereodf>).

(B and C) Fasting-responsive metabolic pathways were plotted in a heatmap, and LFQ intensities were normalized between 0 and 1 on a per-gene basis. Each column represents an individual animal.

(D and E) Individual IFN $\alpha$ / $\beta$ -responsive proteins were also plotted, where each circle is an individual animal, and the boxes represent 95% confidence intervals and whiskers represent 1.5 $\times$  interquartile range. Significance was determined as  $p < 0.05$  by two-way ANOVA after Benjamini-Hochberg correction.

(F) The most significantly changing proteins after EODF with gonadectomy were plotted in a heatmap. LFQ intensities were normalized between 0 and 1 on a per-gene basis. Each column represents an individual animal.

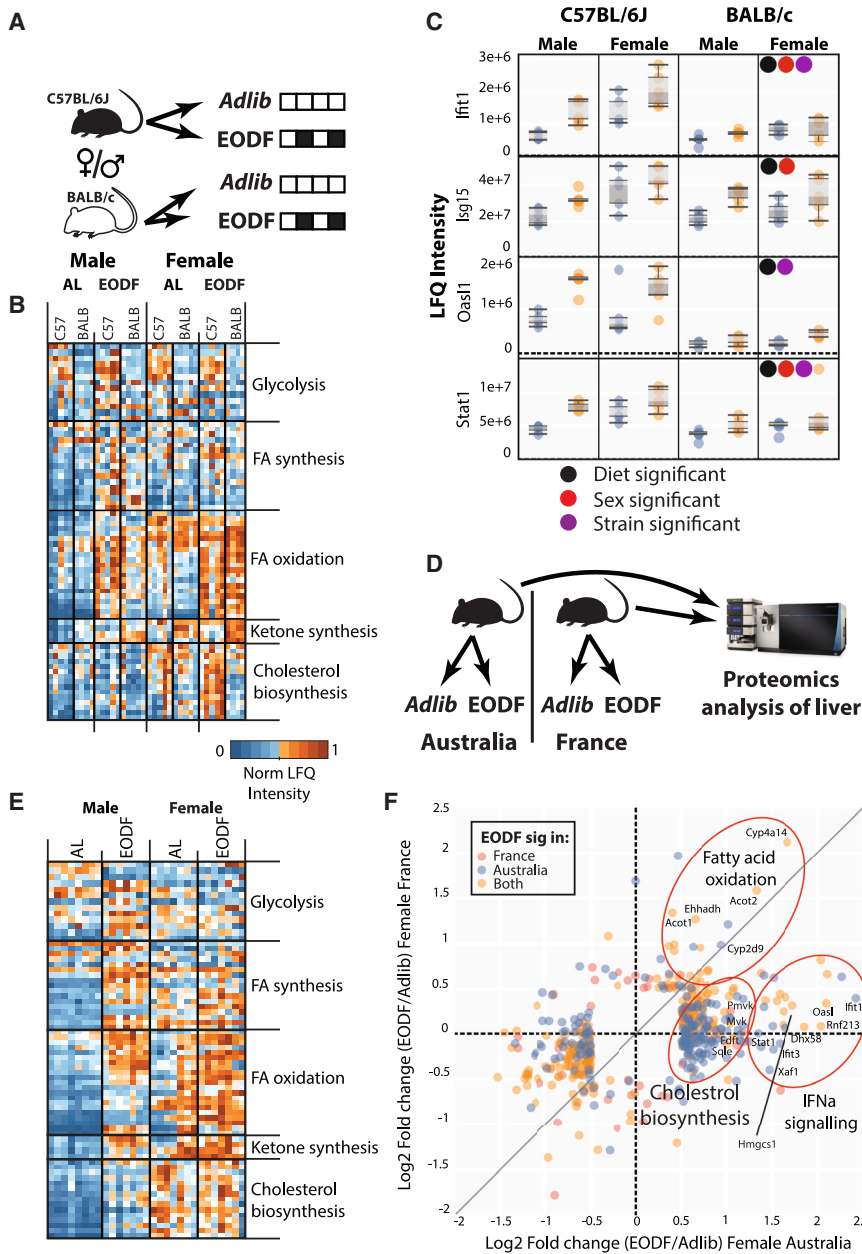


**Figure 6. Genetic background and environmental stimuli affect the magnitude of the EODF-induced IFN $\alpha$  response in mice**

(A) C57BL/6J and BALB/c mice at 8 weeks of age were given either *ad libitum* or EODF food access for 2 weeks, and their organs were harvested after 2 weeks on LN<sub>2</sub> and subjected to tandem mass spectrometry. n = 5 per treatment group.

(B) Fasting-responsive metabolic pathways were plotted in a heatmap, and LFQ intensities were normalized between 0 and 1 on a per-gene basis. Each column represents an individual animal.

(C) Individual ISG proteins were also plotted, where each circle is an individual animal, and the boxes represent 95% confidence intervals and whiskers represent 1.5 $\times$  interquartile range. Significance was determined as p < 0.05 by three-way ANOVA.

(D) Male and female C57BL/6J mice 8 weeks of age were given either *ad libitum* or EODF food access for 2 weeks, and their organs were harvested after 2 weeks on LN<sub>2</sub>. This work was performed at a different facility and compared with previous results. n = 7–8 per treatment group.

(E) Fasting-responsive metabolic pathways were plotted in a heatmap, and LFQ intensities were normalized between 0 and 1 on a per-gene basis. Each column represents an individual animal.

(F) The log<sub>2</sub> fold change (EODF/*ad libitum* [Adlib] in females only) was compared between C57BL/6J mice from facilities in either Australia or France. Only proteins significantly changing in either experiment were plotted, and color indicates within which experiment these proteins were significantly changed.

Unbiased mass-spectrometry-based proteomics enabled us to detect sexual dimorphism in numerous metabolic pathways. Males induced fatty acid synthesis enzymes more than females, whereas females induced fatty acid oxidation and cholesterol biosynthesis more than males. To better understand the role of sex hormone signaling, castrated C57BL/6J mice were subjected to EODF. The EODF response in these mice was more female-like due to increased fatty acid oxidation enzymes. This may suggest that sex hormone signaling can be overcome by nutritional requirements as observed previously.<sup>28</sup> Ovariectomy, on the other hand, had a distinct effect on the EODF response, where cholesterol biosynthesis enzymes were greatly downregulated and fatty acid synthesis enzymes were upregulated

an EODF-induced increase in liver IFN $\alpha$ / $\beta$  signaling that was significantly more pronounced in females. This response was dependent on IFN $\alpha$ / $\beta$  secretion, as KO of the IFN $\alpha$ / $\beta$  receptor IFNAR1 blocked the response. A key trigger for type I IFN production (IFN $\alpha$  and IFN $\beta$ ) is the activation of STING, which can be activated by double-stranded RNA produced during viral replication.<sup>32</sup> However, previous studies have observed nucleic acid-independent activation of the STING pathway through the inhibition of either cholesterol biosynthesis,<sup>33</sup> polyunsaturated fatty acid (PUFA) synthesis, or monounsaturated fatty acid (MUFA) synthesis.<sup>34,35</sup> We have previously shown that fasting significantly decreased the liver protein abundance of key cholesterol biosynthetic enzymes in males, including 3-hydroxy-3-methylglutaryl-

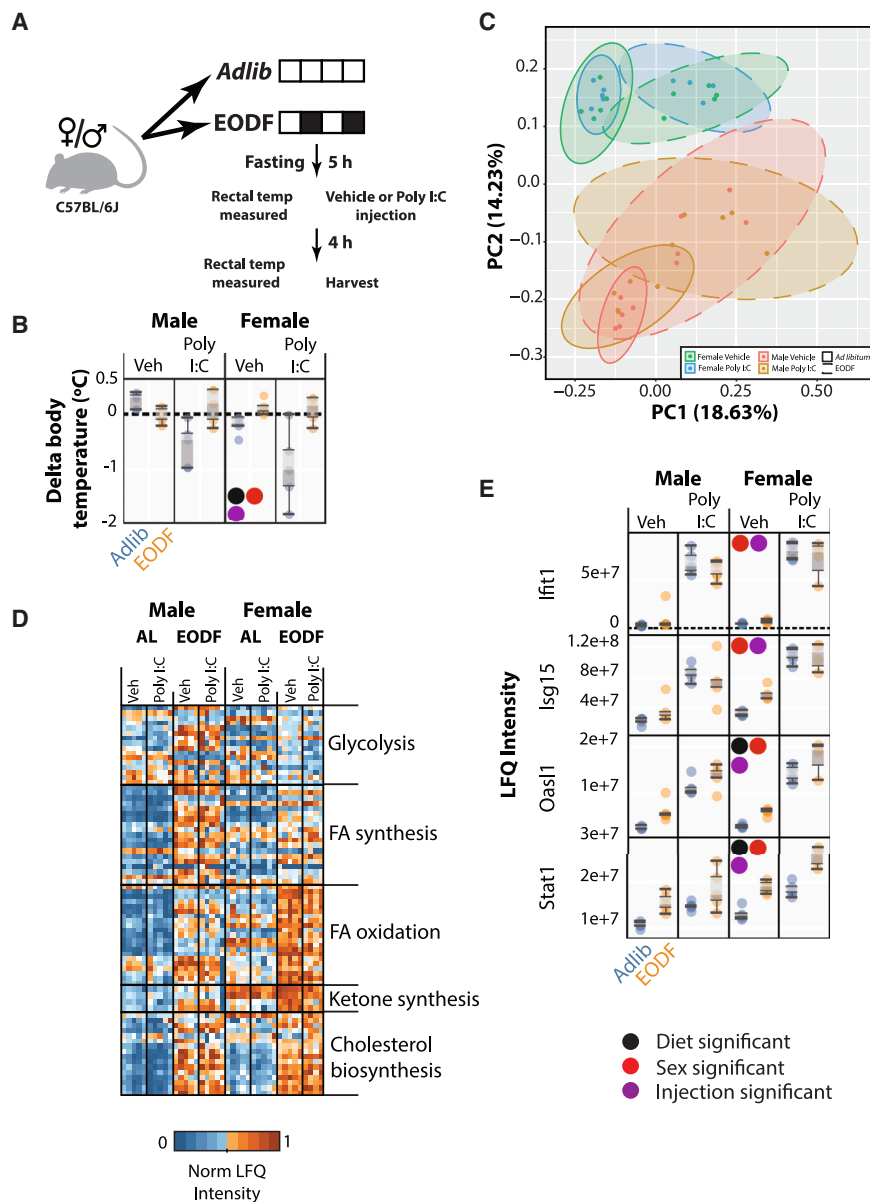


**Figure 7. EODF does not potentiate IFN $\alpha$  signaling in innate immune challenged mice**

(A) Male and female C57BL/6J mice at 8 weeks of age were given either Adlib or EODF food access before injection with the TLR4 agonist polyI:C. Mice were sacrificed 4 h post-injection, and their livers and plasma were harvested and snap frozen using LN<sub>2</sub>. n = 5 per treatment group.

(B) Temperature was monitored rectally before, during, and at the end of the injection period and the delta from beginning to end plotted, where each circle represents an individual animal, and the boxes represent 95% confidence intervals and whiskers represent 1.5 $\times$  interquartile range. Significance was determined as p < 0.05 by three-way ANOVA.

(C) Proteins that were detected in every sample were subject to PCA, where each circle represents an individual animal.

(D) Fasting-responsive metabolic pathways were plotted in a heatmap, and LFQ intensities were normalized between 0 and 1 on a per-gene basis. Each column represents an individual animal.

(E) Individual IFN $\alpha$ -responsive proteins were also plotted, where each circle is an individual animal.

previously shown to affect the gut microbiota in mice, which may affect their metabolic adaptation to EODF.<sup>36,37</sup>

The androgen receptor is known to interact with the IFN $\alpha/\beta$  pathway<sup>38–41</sup> and could be responsible for the sexual dimorphism observed in the liver's response to EODF. In this study, castrated males had a stronger IFN $\alpha$  response than their sham littermates, which is consistent with prior studies showing testosterone specifically inhibits type I IFN responses.<sup>42,43</sup> Interestingly, the protein most negatively regulated by castration was IFN-regulatory factor 2 (IRF2), which is known to dampen type I interferon responses and whose activity can be influenced by the androgen receptor.<sup>44,45</sup> Castrated animals also had

increased cholesterol biosynthesis, which would lead to increased flux during the fasting period and may further contribute to the increased IFN $\alpha/\beta$  signaling. The converse experiment in ovariectomized females had two interesting outcomes. Firstly, *ad libitum*-fed ovariectomized females had reduced ISG protein abundance and cholesterol biosynthesis enzymes compared with their sham counterparts, suggesting that estrogen is directly regulating these proteins. This fits with prior observations that show females have a stronger immunological response in the liver and are more prone to autoimmune disease.<sup>7,46–48</sup> Secondly, the magnitude of ISG protein induction after EODF was unchanged, which showed that while estrogen controls the steady-state levels of ISG proteins, it is not necessary for their induction by EODF. Therefore, both androgens

coenzyme A reductase (HMGCR).<sup>11</sup> We propose that the repeated fasting bouts during EODF prime the liver for IFN $\alpha$  production through the inhibition of one or more of these pathways. This is supported by our data, which showed that females regulated the cholesterol biosynthetic pathway much more strongly than males. Examining the potential link between these pathways in C57BL/6J versus BALB/c mice, we observed that EODF-treated female BALB/c mice had lower cholesterol biosynthesis enzyme induction than their C57BL/6J counterparts, as well as lower ISG protein induction. This further emphasizes the potential link between these two pathways. Similarly, the C57BL/6J mice raised in another facility on the same diet showed lower cholesterol biosynthesis pathway and ISG protein induction. One key environmental difference was that the mice in France were given acidified water,

and estrogens have an important role in the IFN $\alpha/\beta$  induction after EODF, but neither are solely responsible for the observed effects. One caveat to these experiments is that both testosterone and estrogen will be affected by both castration and ovariectomy and may confound these data.

Given the complex interplay between metabolism and immunity, IF may provide benefit beyond metabolic improvements. Previous research has demonstrated that IF prior to injection of the viral mimetic polyI:C leads to a sustained increase in IFN and pro-inflammatory cytokine secretion into the blood of male C57BL/6J mice.<sup>49</sup> Considering this, we hypothesized that EODF would sensitize the liver to innate immune stimuli leading to potentiated ISG protein induction. However, we found that, for the majority of ISG proteins, there was no potentiation between EODF and polyI:C injections. The large (>10-fold higher) induction of ISG proteins after polyI:C injection compared with the EODF-mediated induction demonstrates that EODF is only generating a mild stimulation of this pathway. The only protein that showed a synergistic response to both EODF and polyI:C injections was STAT1, the upstream transcription factor required for IFN $\alpha/\beta$  pathway induction.<sup>50</sup> The lack of synergistic induction by the combination of EODF and polyI:C injections suggests the IFN $\alpha/\beta$  signaling pathway response is already maximally activated.

In conclusion, this study is a comprehensive proteomic analysis of the liver's response to IF, comparing males and females. Our work highlights key changes in innate immune signaling and fatty acid metabolic pathways that provides a link between diet, sex, and immunity. Future studies should aim to characterize the mice null for the STING-activating metabolic pathways to determine if perturbation of each pathway alone or in combination is sufficient to induce IFN $\alpha/\beta$  production. The interactions we have reported between diet, sex, and the innate immune system may allow for development of specific pharmacological perturbation to facilitate improvements in metabolic health.

### Limitations of the study

This study has some limitations. Firstly, gonadectomy is used to examine the effect of each sex hormone upon the IF response. Within each sex, gonadectomy would lead to a decrease in both male and female sex hormones. Perturbation of estrogen in males and testosterone in females may also contribute to the observed response. Secondly, there are differences in cholesterol metabolism between humans and mice. This may mean that the cholesterol biosynthetic response in humans may differ from that observed in this study. Lastly, this study uses an intense fasting regime that may not completely reflect IF regimes commonly used in humans. Future studies should aim to rectify this by examining the effect of differing lengths of fasting on the observed phenotypes in humans.

### STAR★METHODS

Detailed methods are provided in the online version of this paper and include the following:

- KEY RESOURCES TABLE
- RESOURCE AVAILABILITY

- Lead contact
- Materials availability
- Data and code availability

### ● EXPERIMENTAL MODEL AND SUBJECT DETAILS

- Animal and experimental model ethics
- Mice
- Intermittent fasting models
- Mouse gonadectomy
- PolyI:C immune response testing

### ● METHOD DETAILS

- Body composition determination
- Oral glucose tolerance testing (oGTT)
- Insulin ELISA
- Liver triacyl glyceride (TAG) determination
- Tissue collection
- Plasma non-esterified fatty acid (NEFA) determination
- Tissue lysis
- Sample preparation for protein mass spectrometry
- Protein LC-MS/MS and spectra analysis

### ● QUANTIFICATION AND STATISTICAL ANALYSIS

### SUPPLEMENTAL INFORMATION

Supplemental information can be found online at <https://doi.org/10.1016/j.celrep.2023.112559>.

### ACKNOWLEDGMENTS

M.L. is a Cancer Institute NSW Future Research Leader Fellow. We thank SydneyMS for providing the instrumentation used in this study. N.L.'s laboratory was funded by the Fondation ARC pour la recherche contre le cancer, the Agence Nationale de Recherche sur le SIDA et les Hépatites virales (ANRS: ECTZ117448), La Région Languedoc Roussillon, and the CNRS. For animal experiments conducted in France, we acknowledge the iExplore-RAM animal facility.

### AUTHOR CONTRIBUTIONS

M.L. conceived and supervised the project. D.J.H., M.C., G.E.R., and M.L. performed all the animal experiments. D.J.H. and M.L. performed the proteomics experiments and data analysis. D.J.H., M.C., B.V., M.J.H., and M.L. performed the biochemical assays. B.V. and M.J.H. provided the genetically modified animals. I.K.V. and N.L. performed the animal experiments in France. D.J.H. and M.L. wrote the manuscript.

### DECLARATION OF INTERESTS

The authors declare no competing interests.

Received: July 12, 2022

Revised: March 20, 2023

Accepted: May 8, 2023

### REFERENCES

1. Horstman, A.M., Dillon, E.L., Urban, R.J., and Sheffield-Moore, M. (2012). The role of androgens and estrogens on healthy aging and longevity. *J. Gerontol. A Biol. Sci. Med. Sci.* 67, 1140–1152. <https://doi.org/10.1093/gerona/gjs068>.
2. Kelly, D.M., and Jones, T.H. (2013). Testosterone: a metabolic hormone in health and disease. *J. Endocrinol.* 217, R25–R45. <https://doi.org/10.1530/joe-12-0455>.

3. Mauvais-Jarvis, F., Clegg, D.J., and Hevener, A.L. (2013). The role of estrogens in control of energy balance and glucose homeostasis. *Endocr. Rev.* *34*, 309–338. <https://doi.org/10.1210/er.2012-1055>.
4. McEwen, B.S., and Milner, T.A. (2017). Understanding the broad influence of sex hormones and sex differences in the brain. *J. Neurosci. Res.* *95*, 24–39. <https://doi.org/10.1002/jnr.23809>.
5. Ysraelit, M.C., and Correale, J. (2019). Impact of sex hormones on immune function and multiple sclerosis development. *Immunology* *156*, 9–22. <https://doi.org/10.1111/imm.13004>.
6. Sicree, R.A., Zimmet, P.Z., Dunstan, D.W., Cameron, A.J., Welborn, T.A., and Shaw, J.E. (2008). Differences in height explain gender differences in the response to the oral glucose tolerance test- the AusDiab study. *Diabet. Med.* *25*, 296–302. <https://doi.org/10.1111/j.1464-5491.2007.02362.x>.
7. Klein, S.L. (2012). Sex influences immune responses to viruses, and efficacy of prophylaxis and treatments for viral diseases. *Bioessays* *34*, 1050–1059. <https://doi.org/10.1002/bies.201200099>.
8. Ngo, S.T., Steyn, F.J., and McCombe, P.A. (2014). Gender differences in autoimmune disease. *Front. Neuroendocrinol.* *35*, 347–369. <https://doi.org/10.1016/j.ynrne.2014.04.004>.
9. Menke, A., Casagrande, S., Geiss, L., and Cowie, C.C. (2015). Prevalence of and trends in diabetes among adults in the United States, 1988–2012. *JAMA* *314*, 1021–1029. <https://doi.org/10.1001/jama.2015.10029>.
10. Lonardo, A., Nascimbeni, F., Ballestri, S., Fairweather, D., Win, S., Than, T.A., Abdelmalek, M.F., and Suzuki, A. (2019). Sex differences in nonalcoholic fatty liver disease: state of the art and identification of research gaps. *Hepatology* *70*, 1457–1469. <https://doi.org/10.1002/hep.30626>.
11. Hatchwell, L., Harney, D.J., Cieleish, M., Young, K., Koay, Y.C., O’Sullivan, J.F., and Larance, M. (2020). Multi-omics analysis of the intermittent fasting response in mice identifies an unexpected role for HNF4 $\alpha$ . *Cell Rep.* *30*, 3566–3582.e4. <https://doi.org/10.1016/j.celrep.2020.02.051>.
12. Kim, K.H., Kim, Y.H., Son, J.E., Lee, J.H., Kim, S., Choe, M.S., Moon, J.H., Zhong, J., Fu, K., Lenglin, F., et al. (2017). Intermittent fasting promotes adipose thermogenesis and metabolic homeostasis via VEGF-mediated alternative activation of macrophage. *Cell Res.* *27*, 1309–1326. <https://doi.org/10.1038/cr.2017.126>.
13. Li, G., Xie, C., Lu, S., Nichols, R.G., Tian, Y., Li, L., Patel, D., Ma, Y., Brocker, C.N., Yan, T., et al. (2017). Intermittent fasting promotes white adipose browning and decreases obesity by shaping the gut microbiota. *Cell Metabol.* *26*, 672–685.e4. <https://doi.org/10.1016/j.cmet.2017.08.019>.
14. Xie, K., Neff, F., Markert, A., Rozman, J., Aguilar-Pimentel, J.A., Amarie, O.V., Becker, L., Brommage, R., Garrett, L., Henzel, K.S., et al. (2017). Every-other-day feeding extends lifespan but fails to delay many symptoms of aging in mice. *Nat. Commun.* *8*, 155. <https://doi.org/10.1038/s41467-017-00178-3>.
15. Harney, D.J., Cieleish, M., Chu, R., Cooke, K.C., James, D.E., Stöckli, J., and Larance, M. (2021). Proteomics analysis of adipose depots after intermittent fasting reveals visceral fat preservation mechanisms. *Cell Rep.* *34*, 108804. <https://doi.org/10.1016/j.celrep.2021.108804>.
16. Harney, D.J., Hutchison, A.T., Hatchwell, L., Humphrey, S.J., James, D.E., Hocking, S., Heilbronn, L.K., and Larance, M. (2019). Proteomic analysis of human plasma during intermittent fasting. *J. Proteome Res.* *18*, 2228–2240. <https://doi.org/10.1021/acs.jproteome.9b00090>.
17. Harney, D.J., Hutchison, A.T., Su, Z., Hatchwell, L., Heilbronn, L.K., Hocking, S., James, D.E., and Larance, M. (2019). Small-protein enrichment assay enables the rapid, unbiased analysis of over 100 low abundance factors from human plasma. *Mol. Cell. Proteomics* *18*, 1899–1915. <https://doi.org/10.1074/mcp.TIR119.001562>.
18. Heilbronn, L.K., Civitarese, A.E., Bogacka, I., Smith, S.R., Hulver, M., and Ravussin, E. (2005). Glucose tolerance and skeletal muscle gene expression in response to alternate day fasting. *Obes. Res.* *13*, 574–581. <https://doi.org/10.1038/oby.2005.61>.
19. Sutton, E.F., Beyl, R., Early, K.S., Cefalu, W.T., Ravussin, E., and Peterson, C.M. (2018). Early time-restricted feeding improves insulin sensitivity, blood pressure, and oxidative stress even without weight loss in men with prediabetes. *Cell Metabol.* *27*, 1212–1221.e3. <https://doi.org/10.1016/j.cmet.2018.04.010>.
20. Tinsley, G.M., Moore, M.L., Graybeal, A.J., Paoli, A., Kim, Y., Gonzales, J.U., Harry, J.R., VanDusseldorp, T.A., Kennedy, D.N., and Cruz, M.R. (2019). Time-restricted feeding plus resistance training in active females: a randomized trial. *Am. J. Clin. Nutr.* *110*, 628–640. <https://doi.org/10.1093/ajcn/nqz126>.
21. Mitchell, S.J., Madrigal-Matute, J., Scheibye-Knudsen, M., Fang, E., Aon, M., González-Reyes, J.A., Cortassa, S., Kaushik, S., Gonzalez-Freire, M., Patel, B., et al. (2016). Effects of sex, strain, and energy intake on hallmarks of aging in mice. *Cell Metabol.* *23*, 1093–1112. <https://doi.org/10.1016/j.cmet.2016.05.027>.
22. Brie, B., Ramirez, M.C., De Winne, C., Lopez Vicchi, F., Villarruel, L., Soriano, E., Catalano, P., Ornstein, A.M., and Becu-Villalobos, D. (2019). Brain control of sexually dimorphic liver function and disease: the endocrine connection. *Cell. Mol. Neurobiol.* *39*, 169–180. <https://doi.org/10.1007/s10571-019-00652-0>.
23. Lefebvre, P., and Staels, B. (2021). Hepatic sexual dimorphism - implications for non-alcoholic fatty liver disease. *Nat. Rev. Endocrinol.* *17*, 662–670. <https://doi.org/10.1038/s41574-021-00538-6>.
24. Milette, S., Hashimoto, M., Perrino, S., Qi, S., Chen, M., Ham, B., Wang, N., Istomine, R., Lowy, A.M., Piccirillo, C.A., and Brodt, P. (2019). Sexual dimorphism and the role of estrogen in the immune microenvironment of liver metastases. *Nat. Commun.* *10*, 5745. <https://doi.org/10.1038/s41467-019-13571-x>.
25. Szklarczyk, D., Kirsch, R., Koutrouli, M., Nastou, K., Mehryary, F., Hachilif, R., Gable, A.L., Fang, T., Doncheva, N.T., Pyysalo, S., et al. (2023). The STRING database in 2023: protein-protein association networks and functional enrichment analyses for any sequenced genome of interest. *Nucleic Acids Res.* *51*, D638–d646. <https://doi.org/10.1093/nar/gkac1000>.
26. Yamauchi, T., Kamon, J., Waki, H., Terauchi, Y., Kubota, N., Hara, K., Mori, Y., Ide, T., Murakami, K., Tsuboyama-Kasaoka, N., et al. (2001). The fat-derived hormone adiponectin reverses insulin resistance associated with both lipodystrophy and obesity. *Nat. Med.* *7*, 941–946. <https://doi.org/10.1038/90984>.
27. Platanius, L.C. (2005). Mechanisms of type-I- and type-II-interferon-mediated signalling. *Nat. Rev. Immunol.* *5*, 375–386. <https://doi.org/10.1038/nri1604>.
28. Kelly, D.M., Nettleship, J.E., Akhtar, S., Muraleedharan, V., Sellers, D.J., Brooke, J.C., McLaren, D.S., Channer, K.S., and Jones, T.H. (2014). Testosterone suppresses the expression of regulatory enzymes of fatty acid synthesis and protects against hepatic steatosis in cholesterol-fed androgen deficient mice. *Life Sci.* *109*, 95–103. <https://doi.org/10.1016/j.lfs.2014.06.007>.
29. Gao, H., Fält, S., Sandelin, A., Gustafsson, J.A., and Dahlman-Wright, K. (2008). Genome-wide identification of estrogen receptor alpha-binding sites in mouse liver. *Mol. Endocrinol.* *22*, 10–22. <https://doi.org/10.1210/me.2007-0121>.
30. Parks, B.W., Sallam, T., Mehrabian, M., Psychogios, N., Hui, S.T., Nozheim, F., Castellani, L.W., Rau, C.D., Pan, C., Phun, J., et al. (2015). Genetic architecture of insulin resistance in the mouse. *Cell Metabol.* *21*, 334–347. <https://doi.org/10.1016/j.cmet.2015.01.002>.
31. Zhang, Y., Klein, K., Sugathan, A., Nassery, N., Dombkowski, A., Zanger, U.M., and Waxman, D.J. (2011). Transcriptional profiling of human liver identifies sex-biased genes associated with polygenic dyslipidemia and coronary artery disease. *PLoS One* *6*, e23506. <https://doi.org/10.1371/journal.pone.0023506>.
32. Barber, G.N. (2015). STING: infection, inflammation and cancer. *Nat. Rev. Immunol.* *15*, 760–770. <https://doi.org/10.1038/nri3921>.
33. York, A.G., Williams, K.J., Argus, J.P., Zhou, Q.D., Brar, G., Vergnes, L., Gray, E.E., Zhen, A., Wu, N.C., Yamada, D.H., et al. (2015). Limiting cholesterol biosynthetic flux spontaneously engages type I IFN signaling. *Cell* *163*, 1716–1729. <https://doi.org/10.1016/j.cell.2015.11.045>.

34. Kanno, T., Nakajima, T., Yokoyama, S., Asou, H.K., Sasamoto, S., Kamii, Y., Hayashizaki, K., Ouchi, Y., Onodera, T., Takahashi, Y., et al. (2021). SCD2-mediated monounsaturated fatty acid metabolism regulates cGAS-STING-dependent type I IFN responses in CD4(+) T cells. *Commun. Biol.* *4*, 820. <https://doi.org/10.1038/s42003-021-02310-y>.
35. Vila, I.K., Chamma, H., Steer, A., Saccas, M., Taffoni, C., Turtoi, E., Reinert, L.S., Hussain, S., Marines, J., Jin, L., et al. (2022). STING orchestrates the crosstalk between polyunsaturated fatty acid metabolism and inflammatory responses. *Cell Metabol.* *34*, 125–139.e8. <https://doi.org/10.1016/j.cmet.2021.12.007>.
36. Hall, J.E., White, W.J., and Lang, C.M. (1980). Acidification of drinking water: its effects on selected biologic phenomena in male mice. *Lab. Anim. Sci.* *30*, 643–651.
37. Whipple, B., Agar, J., Zhao, J., Pearce, D.A., and Kovács, A.D. (2021). The acidified drinking water-induced changes in the behavior and gut microbiota of wild-type mice depend on the acidification mode. *Sci. Rep.* *11*, 2877. <https://doi.org/10.1038/s41598-021-82570-0>.
38. Asirvatham, A.J., Schmidt, M., Gao, B., and Chaudhary, J. (2006). Androgens regulate the immune/inflammatory response and cell survival pathways in rat ventral prostate epithelial cells. *Endocrinology* *147*, 257–271. <https://doi.org/10.1210/en.2005-0942>.
39. Kovats, S. (2015). Estrogen receptors regulate innate immune cells and signaling pathways. *Cell. Immunol.* *294*, 63–69. <https://doi.org/10.1016/j.cellimm.2015.01.018>.
40. Laffont, S., Rouquié, N., Azar, P., Seillet, C., Plumas, J., Aspod, C., and Guéry, J.C. (2014). X-Chromosome complement and estrogen receptor signaling independently contribute to the enhanced TLR7-mediated IFN- $\alpha$  production of plasmacytoid dendritic cells from women. *J. Immunol.* *193*, 5444–5452. <https://doi.org/10.4049/jimmunol.1303400>.
41. Lai, J.J., Lai, K.P., Zeng, W., Chuang, K.H., Altuwajri, S., and Chang, C. (2012). Androgen receptor influences on body defense system via modulation of innate and adaptive immune systems: lessons from conditional AR knockout mice. *Am. J. Pathol.* *181*, 1504–1512. <https://doi.org/10.1016/j.ajpath.2012.07.008>.
42. Rettew, J.A., Huet-Hudson, Y.M., and Marriott, I. (2008). Testosterone reduces macrophage expression in the mouse of toll-like receptor 4, a trigger for inflammation and innate immunity. *Biol. Reprod.* *78*, 432–437. <https://doi.org/10.1095/biolreprod.107.063545>.
43. Webb, K., Peckham, H., Radziszewska, A., Menon, M., Oliveri, P., Simpson, F., Deakin, C.T., Lee, S., Ciurtin, C., Butler, G., et al. (2018). Sex and pubertal differences in the type 1 interferon pathway associate with both X chromosome number and serum sex hormone concentration. *Front. Immunol.* *9*, 3167. <https://doi.org/10.3389/fimmu.2018.03167>.
44. Kikuchi, M., Okumura, F., Tsukiyama, T., Watanabe, M., Miyajima, N., Tanaka, J., Imamura, M., and Hatakeyama, S. (2009). TRIM24 mediates ligand-dependent activation of androgen receptor and is repressed by a bromodomain-containing protein, BRD7, in prostate cancer cells. *Biochim. Biophys. Acta* *1793*, 1828–1836. <https://doi.org/10.1016/j.bbamcr.2009.11.001>.
45. Staal, A., Enserink, J.M., Stein, J.L., Stein, G.S., and van Wijnen, A.J. (2000). Molecular characterization of celtix-1, a bromodomain protein interacting with the transcription factor interferon regulatory factor 2. *J. Cell. Physiol.* *185*, 269–279. <https://doi.org/10.1002/1097-4652>.
46. Bakr, I., Rekecawicz, C., El Hosseiny, M., Ismail, S., El Daly, M., El-Kafrawy, S., Esmat, G., Hamid, M.A., Mohamed, M.K., and Fontanet, A. (2006). Higher clearance of hepatitis C virus infection in females compared with males. *Gut* *55*, 1183–1187. <https://doi.org/10.1136/gut.2005.078147>.
47. Klein, S.L., and Flanagan, K.L. (2016). Sex differences in immune responses. *Nat. Rev. Immunol.* *16*, 626–638. <https://doi.org/10.1038/nri.2016.90>.
48. Wang, S.-H., Chen, P.-J., and Yeh, S.-H. (2015). Gender disparity in chronic hepatitis B: mechanisms of sex hormones. *J. Gastroenterol. Hepatol.* *30*, 1237–1245. <https://doi.org/10.1111/jgh.12934>.
49. Zenz, G., Jačan, A., Reichmann, F., Farzi, A., and Holzer, P. (2019). Intermittent fasting exacerbates the acute immune and behavioral sickness response to the viral mimic poly(I:C) in mice. *Front. Neurosci.* *13*, 359. <https://doi.org/10.3389/fnins.2019.00359>.
50. McNab, F., Mayer-Barber, K., Sher, A., Wack, A., and O'Garra, A. (2015). Type I interferons in infectious disease. *Nat. Rev. Immunol.* *15*, 87–103. <https://doi.org/10.1038/nri3787>.
51. Müller, U., Steinhoff, U., Reis, L.F., Hemmi, S., Pavlovic, J., Zinkernagel, R.M., and Aguet, M. (1994). Functional role of type I and type II interferons in antiviral defense. *Science* *264*, 1918–1921. <https://doi.org/10.1126/science.8009221>.
52. Demichev, V., Messner, C.B., Vernardis, S.I., Lilley, K.S., and Ralser, M. (2020). DIA-NN: neural networks and interference correction enable deep proteome coverage in high throughput. *Nat. Methods* *17*, 41–44. <https://doi.org/10.1038/s41592-019-0638-x>.

## STAR★METHODS

### KEY RESOURCES TABLE

REAGENT or RESOURCE	SOURCE	IDENTIFIER
<b>Chemicals, peptides, and recombinant proteins</b>		
Water	Thermo Fisher Scientific	Cat# FSBW6-4
Acetonitrile	Thermo Fisher Scientific	Cat# FSBA955-4
Ethyl acetate	Merck Millipore	Cat# 109623
Triscarboxyethylphosphine (TCEP) (Neutral pH solution)	Thermo Fisher Scientific	Cat# 77720
Chloracetamide (CAA)	Sigma Aldrich	Cat# C0267
Trypsin	ThermoFisher Scientific	90059
Sodium deoxycholate	Sigma Aldrich	D6750
Styrenedivinylbenzene reversed phase sulfonate (SDB-RPS)	Merck Millipore	66886-U
Triglyceride reagent	ThermoFisher Scientific	TR22421
Glycerol	Precimat	Cat# 10166588
<b>Critical commercial assays</b>		
BCA total protein assay kit	Thermo Fisher Scientific	Cat# 23225
Insulin ELISA	Crystal Chem	Cat# 90080
Non-esterified fatty acid (NEFA) quantification kit	FujiFilm - Wako	Cat# NEFAC-279-75401
<b>Deposited data</b>		
Proteomic data from this study	ProteomeXchange Consortium	PXD034823
<b>Experimental models: Organisms/strains</b>		
C57BL/6J mice (male and female)	Australian BioResources and Australian Resources Center	C57BL/6J
BALB/c mice (male and female)	Australian Resources Center	BALB/c
IFNAR1 K/O mice on C57BL/6J background	Markus Hofer	IFNAR1 K/O
<b>Software and algorithms</b>		
DIA-NN	<a href="https://github.com/vdemichev/DiaNN">https://github.com/vdemichev/DiaNN</a>	Version 1.8
R	R project	Version 3.6.1
Tableau desktop	Tableau	Version 2023.1

### RESOURCE AVAILABILITY

#### Lead contact

Information and requests for reagents and resources should be directed to and will be fulfilled by the lead contact, Mark Larence ([mark.larence@sydney.edu.au](mailto:mark.larence@sydney.edu.au)).

#### Materials availability

This study did not generate new unique reagents.

#### Data and code availability

The proteomic datasets generated during this study have been deposited to the ProteomeXchange Consortium ([proteomexchange.org](http://proteomexchange.org)) via the PRIDE partner repository with the dataset identifier PRIDE: PXD034823. These data are publicly available as of the data of publication.

This paper does not report original code.

Any additional information required to reanalyze the data reported in this paper is available from the [lead contact](#) upon request.

## EXPERIMENTAL MODEL AND SUBJECT DETAILS

### Animal and experimental model ethics

All data contained in this manuscript was derived from experiments performed with the approval of the University of Sydney Animal Ethics Committee (2020/1893), which adheres to the National Health and Medical Research Council of Australia and ARRIVE guidelines.

Animal protocols were performed in accordance with French and European Animal Care Facility guidelines. All experiments were approved by the Animal Welfare and Ethical Review Body of Languedoc-Roussillon. Housing and experimental procedures were approved by the French Agriculture and Forestry Ministry (animal facility agreement A34-172-13, ethics committee 1521-16673 & protocol number 2018090715484364).

### Mice

All wildtype C57BL/6J mice were supplied by either Australian Bio-Resources (Moss Vale, Australia) or Australian Resources Center (Canning Vale, Australia). All wildtype BALB/c mice were supplied by Australian Resources Center. Interferon alpha receptor 1 (IFNAR1) KO mice on a C57BL/6J lineage were previously described.<sup>51</sup> Mice were housed in groups of 2–5 in IVC cages on corn cob bedding (Bed-o’Cobs, Andersons, Maumee, USA). Prior to beginning the intermittent fasting model, all mice were acclimated for a minimum of 1 week. Rooms for housing were temperature-controlled (22°C) with a 12 h light/dark cycle (0600/1800 h). Mice were provided *Ad Libitum* food (standard chow consisting of 12% calories derived from fat; 23% calories derived from protein and 65% calories derived from carbohydrates [Specialty Feeds, Australia], [Table S4](#)) and water access.

### Intermittent fasting models

Male and female mice between 9 and 12 weeks of age were randomly assigned to either *ad libitum*, or every-other-day fasting (EODF) dietary groups on a per cage basis. Cage bedding was switched to paper bedding (Pure-o’Cel, Andersons) throughout the model. EODF mice alternated between *ad libitum* food and water access and complete deprived of food with *ad libitum* water access at 1200 h with cages changed upon fasting induction. *Ad libitum* control mice cages were changed at the same time. At this time, each mouse weight was recorded individually, and food consumption was recorded on a per cage basis. Body composition analysis occurred on model day 8 and oral blood glucose analysis occurred on model day 10. Model termination occurred after 12 days with tissue collection occurring between 0800 and 1030 h after overnight *ad libitum* feeding.

### Mouse gonadectomy

Testicles in males were accessed through the abdominal cavity and blood supply to testicle limited by hemostat. Blood vessels were cauterized and whole testicle were removed from both sides. Muscle layers were sutured post testicle removal. Sham animals had identical incisions, but no organs were removed.

Ovaries in females were accessed through abdominal cavity and blood supply limited to ovaries by hemostat. Blood vessels were cauterized and whole ovaries were removed from both sides. Muscle layers were sutured post ovary removal. Sham animals had identical incisions, but no organs were removed.

### Poly:I:C immune response testing

Male and female C57BL/6J mice were placed run on the EODF protocol described in “[Intermittent fasting models](#).” Following the completion of the model, mice were given *ad libitum* access to food and water overnight. Food was removed at 6am (when lights are turned on). After 5 h of fasting, temperature was taken rectally (BAT-12 microprobe thermometer, PhysiTemp). Mice were either injected with water or Poly I:C (12 mg/kg, Invivogen, Cat No. tlr-picw). Animals were monitored hourly for 4 h following which temperature was taken rectally again and then sacrificed.

## METHOD DETAILS

### Body composition determination

Body composition was determined after a night with *ad libitum* food access. Body mass (fat and lean mass) was measured between 0800 and 1000 h by magnetic resonance imaging (MRI) using an EchoMRI-900 analyzer (EchoMRI, Houston, USA) according to manufacturer’s instructions.

### Oral glucose tolerance testing (oGTT)

Mice were fasted for 5 h from 0800 h, after overnight feeding with *ad libitum* food access. At –90 m, mice were transferred to procedure room and allowed to acclimate. At –15 m, fasting blood glucose (Accu-Chek II glucometer, Roche Diagnostics) and fasting blood ketone bodies (FreeStyle Optimum Neo ketone reader, Abbott) concentrations were measured by whole blood sampling from tail tip incision. At this time whole blood was harvested for an insulin ELISA as below. Glucose was administered orally by gavage at 2 g/kg (25% v/v solution) per lean mass as determined by MRI two days prior. Blood glucose was monitored at regular time intervals for 90 m by whole blood sampling from same tail tip incision.

### Insulin ELISA

Whole blood was collected as described in oral glucose tolerance testing and diluted into insulin ELISA plate (Crystal Chem, Illinois, USA) which was incubated overnight at 4°C. Insulin ELISA was conducted as per the manufacturer's instructions and read using a Tecan infinite M200 pro plate reader (Tecan, Switzerland).

### Liver triacyl glyceride (TAG) determination

Liver tissue frozen on liquid nitrogen was pulverized and extracted in methanol and chloroform (1:2). Liver was extracted for at least 2h while rotating. Sodium chloride was added at final concentration of 0.4%. Samples were centrifuged for 10 min at 2000 x g at RT. The bottom layer was recovered and evaporated. Dried samples were resuspended in absolute ethanol. Liver TAGs were measured with absorbance at 490nm with triglyceride reagent (ThermoFisher, Cat# TR22421). Triglyceride and glycerol standards were used. Absorbance was measured using a Tecan M200 pro plate reader.

### Tissue collection

Mice were sacrificed between 0850 and 1050 h using CO<sub>2</sub> suffocation. Whole blood was collected by cardiac puncture then liver tissue was excised. Whole blood was mixed with protease inhibitors (100 μM vildagliptin and 50 mM benzamidine) and 50 mM EDTA and kept on ice. At the conclusion of tissue collection, whole blood was spun at 1,500 x g for 15 min at 4°C, plasma collected and snap frozen in LN<sub>2</sub>. Liver tissue was immediately snap frozen using freeze clamps (made in-house) frozen in LN<sub>2</sub>. All tissues were stored at -80°C.

### Plasma non-esterified fatty acid (NEFA) determination

Plasma was collected as in tissue collection and defrosted on ice. NEFAs were measured according to manufacturer's instructions (Cat No. 279-75401, FujiFilm - Wako, Japan). Absorbance was measured using a Tecan M200pro plate reader.

### Tissue lysis

Frozen tissue was lysed in 4% sodium deoxycholate (SDC) and 100mM tris-HCl (pH 7.5) at RT using an Ultra-Turrax T8 stick homogenizer (IKA, Werke) at an intensity of 2 for 30 s. Lysates were immediately heated to 65°C for 10 m with shaking. After cooling to RT, lysates were sonicated at 70% amplitude for 10 m using 10:10 s pulses at RT using a Q800R2 sonicator (QSonica, Connecticut, USA). Lysates were spun at 18,000 x g for 10 m at RT. Neutral lipid layer was aspirated and supernatant collected while avoiding any pellet.

### Sample preparation for protein mass spectrometry

Protein concentration was determined using a BCA total protein assay (Pierce) according to the manufacturer's instructions. Proteins were reduced using 10mM TCEP and alkylated using 40mM chloroacetamide simultaneously at 95°C for 1h. Samples were diluted to 1% SDC using 100mM tris-HCl (pH 8) and digested for 16 h using MS-grade trypsin (stored in 50mM acetic acid) at a ratio of 1:50 trypsin to protein at 37°C with constant shaking. Peptide samples were diluted with 99% ethyl acetate & 1% trifluoroacetic acid (TFA) (50% final concentration, v/v) and allowed to shake until all SDC precipitants were resuspended. Sample clean-up was performed as previously reported<sup>17</sup> except only the bottom aqueous phase of the sample was used in the StageTips. Following centrifugal evaporation, peptides were resuspended in 5% formic acid and stored at 4°C before LC-MS/MS acquisition.

### Protein LC-MS/MS and spectra analysis

Peptides prepared as above, were directly injected onto a 40cm x 70 μm C18 (Dr. Maisch, Ammerbuch, Germany, 1.9 μm) fused silica analytical column with a 10 μm pulled tip, coupled online to a nanospray ESI source. Peptides were resolved over a gradient from 7%–35% acetonitrile over 120 min with a flow rate of 300 nL min<sup>-1</sup>. Peptide ionization by electrospray occurred at 2.3 kV. A Q-Exactive Fusion Lumos or Q-Exactive Fusion Eclipse mass spectrometer (ThermoFisher) with HCD fragmentation was used for MS/MS acquisition. Spectra were obtained in a data-independent acquisition using 20 variable isolation width search windows. RAW data files were analyzed using the quantitative DIA proteomics search engine, DIA-NN (version 1.8).<sup>52</sup> The output of the DIANN searches was uploaded to the ProteomeXchange Consortium under the identifier PXD034823. For library generation, the Uniprot mouse Swissprot database downloaded on the seventh of May 2021 was used. Fully specific trypsin was set as the protease allowing for 1 missed cleavage and 1 variable modification. Protein N terminus acetylation and oxidation of methionine were set as variable modifications. Carbamidomethylation of cystine was set as a fixed modification. Remove likely interferences and match between runs were enabled. Neural network classifier was set to single-pass mode. Protein inference was based on genes. Quantification strategy was set to any LC (high accuracy). Cross-run normalization was set to RT-dependent. Library profiling was set to full profiling. Data was processed as in statistical analysis.

## QUANTIFICATION AND STATISTICAL ANALYSIS

Proteomics data was analyzed in R (version 3.6.1) and visualized in Tableau (version 2023.1). Fold changes were calculated on a per group basis, based on median values. Statistical significance was determined using either a two- (Sex vs. Diet or Intervention vs. Diet) or three-way (Sex vs. Diet vs. Genotype/Strain/Injection) ANOVA. Statistical outputs were corrected for multiple hypothesis testing using the Benjamini-Hochberg correction, with significance being set at  $p < 0.05$  at an FDR of 5%.